RC25199 (W1108-019) August 2, 2011 (updated 5/3/13)
Mathematics

IBM Research Report

Quantile Periodograms

Ta-Hsin Li
IBM Research Division
Thomas J. Watson Research Center
P.O. Box 218
Yorktown Heights, NY 10598
thl@us.ibm.com

Research Division
Almaden - Austin - Beijing - Cambridge - Haifa - India - T. J. Watson - Tokyo - Zurich

Quantile Periodograms

(Complete Version)

Ta-Hsin Li

IBM T. J. Watson Research Center

Yorktown Heights, NY 10598-0218, USA

(thl@us.ibm.com)

March 9, 2012

Abstract

Two periodogram-like functions, called quantile periodograms, are introduced for spectral analysis of time series. The quantile periodograms are constructed from trigonometric quantile regression and motivated by different interpretations of the ordinary periodogram. Analytical and numerical results demonstrate the capability of the quantile periodograms for detecting hidden periodicity in the quantiles and for providing an additional view of time-series data. A connection between the quantile periodograms and the so-called level-crossing spectrum is established through an asymptotic analysis.

Key Words and Phrases: Fourier transform, hidden periodicity, level crossing, periodogram, power spectrum, quantile regression, spectral analysis, time series.

Version History: (1) April 10, 2011; (2) July 30, 2011; (3) October 4, 2011; (4) March 9, 2012

1. Introduction

Quantile regression is a powerful method that extends the capability of conventional least-squares techniques and enriches the arsenal of statistical procedures for data analysis in a wide range of applications (Koenker 2005). Unlike the conventional regression methods which focus on the conditional mean, quantile regression examines the conditional quantiles and thereby provides a much broader view of the data. Inspired by its success in solving regression problems, we employ the quantile regression technique to define two periodogram-like functions, called the quantile periodograms of the first and second kind, for Fourier spectral analysis of time-series data.

The quantile periodograms can be viewed as generalizations of the ordinary periodogram, which has been widely used in many applications (Bloomfield 2000), and of its robust alternative, the Laplace periodogram, which was discussed more recently (Li 2008, 2012). This paper demonstrates that the quantile periodograms not only share the property of the ordinary periodogram as a frequency-domain representation of serial dependence of the underlying random process, but also offer a much richer view of the time-series data than the one provided by the ordinary periodogram. More specifically, we show that the quantile periodograms are able to detect hidden periodicity in the quantiles. We also show that the quantile periodograms are able to uncover quantile-dependent spectral properties that cannot be seen from the ordinary periodogram. An asymptotic analysis connects the quantile periodograms to what we call the level-crossing spectrum as a frequency-domain representation of serial dependence for random processes.

2. Quantile Periodograms

Given $\alpha \in (0,1)$, define a nonnegative function $\rho_\alpha(u)$ for $u \in \mathbb{R}$ as

$$\rho_\alpha(u) := u\{\alpha - I(u<0)\} = \begin{cases} -(1-\alpha)u & \text{if } u < 0, \\ \alpha u & \text{if } u \geq 0, \end{cases}$$

where $I(\cdot)$ is the indicator function. The sample α-quantile of a real-valued time series $\{Y_1,\ldots,Y_n\}$, denoted by $\hat{\lambda}_n$, minimizes the cost function $\sum_{t=1}^{n}\rho_\alpha(Y_t-\lambda)$ (Koenker 2005, p. 7). In other words, we can write

$$\hat{\lambda}_n := \arg\min_{\lambda\in\mathbb{R}} \sum_{t=1}^{n} \rho_\alpha(Y_t-\lambda). \tag{1}$$

More generally, a linear quantile regression solution is given by minimizing

$$\sum_{t=1}^{n} \rho_\alpha(Y_t-\mathbf{x}_t^T\boldsymbol{\beta}),$$

where $\mathbf{x}_t$ denotes the vector of regressors (or covariates). Linear programming techniques can be used to compute the solution (Koenker 2005, Chapter 6; Portnoy and Koenker 1997).

The underlying assumption in quantile regression is that the α-quantile of Y_t, denoted as λ_t, has a linear relationship with the regressor, i.e., $\lambda_t=\mathbf{x}_t^T\boldsymbol{\beta}_0$ for some $\boldsymbol{\beta}_0\neq\mathbf{0}$. In this paper, we are interested in situations where the quantile contains hidden periodicity. A simple example is

$$Y_t = a_t X_t \qquad (t=1,\ldots,n), \tag{2}$$

where $\{X_t\}$ is a stationary random process and $\{a_t\}$ is a nonnegative periodic sequence of the form

$$a_t = b_0 + b_1\cos(\omega_0 t) + b_2\sin(\omega_0 t) \qquad (0<\omega_0<\pi).$$

Such multiplicative seasonality models can be found in econometric and other applications. With c denoting the α-quantile of X_t in (2), it is easy to show that $\lambda_t = ca_t = \lambda + \mathbf{x}_t^T(\omega_0)\boldsymbol{\beta}_0$, where $\lambda := cb_0$, $\mathbf{x}_t(\omega_0) := [\cos(\omega_0 t),\sin(\omega_0 t)]^T$, and $\boldsymbol{\beta}_0 := [cb_1, cb_2]^T$. To detect the hidden periodicity, it is natural to take a trigonometric regressor $\mathbf{x}_t(\omega) := [\cos(\omega t),\sin(\omega t)]^T$ and consider the linear trigonometric quantile regression solution

$$\hat{\boldsymbol{\beta}}_n(\omega) := \arg\min_{\boldsymbol{\beta}\in\mathbb{R}^2} \sum_{t=1}^{n} \rho_\alpha(Y_t-\lambda-\mathbf{x}_t^T(\omega)\boldsymbol{\beta}), \tag{3}$$

where $\omega := 2\pi f \in (0,\pi)$ is the frequency variable and λ is a suitable constant, typically the α-quantile of $\{Y_t\}$. We define the quantile periodogram of the first kind (or the quantile periodogram I) as

$$Q_{n,\mathrm{I}}(\omega) := \frac{1}{4} n \|\hat{\boldsymbol{\beta}}_n(\omega)\|_2^2, \tag{4}$$

where $\|\cdot\|_2$ denotes the ℓ_2 norm of vectors. We define the quantile periodogram of the second kind (or the quantile periodogram II) as

$$Q_{n,\mathrm{II}}(\omega) := \sum_{t=1}^{n} \{\rho_\alpha(Y_t - \lambda) - \rho_\alpha(Y_t - \lambda - \mathbf{x}_t^T(\omega)\hat{\boldsymbol{\beta}}_n(\omega))\}. \tag{5}$$

Both quantile periodograms measure the contribution of the trigonometric regressor: the quantile periodogram I examines the total power of the trigonometric regressor, whereas the quantile periodogram II considers the net effect of the trigonometric regressor on the cost function.

While the parameter λ is fixed in (3), it can also be optimized together with $\boldsymbol{\beta}$ to yield the extended quantile regression solution

$$\{\hat{\lambda}_n(\omega), \hat{\boldsymbol{\beta}}_n(\omega)\} := \arg \min_{\lambda \in \mathbb{R}, \boldsymbol{\beta} \in \mathbb{R}^2} \sum_{t=1}^{n} \rho_\alpha(Y_t - \lambda - \mathbf{x}_t^T(\omega)\boldsymbol{\beta}). \tag{6}$$

In this case, the quantile periodogram I retains the form in (4), but the corresponding quantile periodogram II takes a slightly modified form

$$Q_{n,\mathrm{II}}(\omega) := \sum_{t=1}^{n} \{\rho_\alpha(Y_t - \hat{\lambda}_n) - \rho_\alpha(Y_t - \hat{\lambda}_n(\omega) - \mathbf{x}_t^T(\omega)\hat{\boldsymbol{\beta}}_n(\omega))\}, \tag{7}$$

where $\hat{\lambda}_n$ is the sample quantile given by (1).

With the special choice of $\alpha = 1/2$ (median or least-absolute-deviations regression), the quantile periodograms reduce to the Laplace periodograms discussed in Li (2008, 2012). Like the Laplace periodograms, the quantile periodograms can be regarded as generalizations of the ordinary periodogram

$$I_n(\omega) := n^{-1} \left| \sum_{t=1}^{n} Y_t \exp(-it\omega) \right|^2.$$

Indeed, at the Fourier frequencies where ω is an integral multiple of $2\pi/n$, it is easy to show that

$$I_n(\omega) = \frac{1}{4} n \|\bar{\boldsymbol{\beta}}_n(\omega)\|_2^2, \tag{8}$$

where $\bar{\boldsymbol{\beta}}_n(\omega)$ is the solution to the linear trigonometric least-squares regression problem

$$\bar{\boldsymbol{\beta}}_n(\omega) := \arg \min_{\boldsymbol{\beta} \in \mathbb{R}^2} \sum_{t=1}^{n} \tfrac{1}{2} |Y_t - \lambda - \mathbf{x}_t^T(\omega)\boldsymbol{\beta}|^2.$$

One can also obtain $\bar{\boldsymbol{\beta}}_n(\omega)$ from the extended least-squares regression problem

$$\{\bar{\lambda}_n, \bar{\boldsymbol{\beta}}_n(\omega)\} := \arg \min_{\lambda \in \mathbb{R}, \boldsymbol{\beta} \in \mathbb{R}^2} \sum_{t=1}^{n} \tfrac{1}{2} |Y_t - \lambda - \mathbf{x}_t^T(\omega)\boldsymbol{\beta}|^2,$$

where $\bar{\lambda}_n$ is nothing but the sample mean which satisfies

$$\bar{\lambda}_n = \arg \min_{\lambda \in \mathbb{R}} \sum_{t=1}^{n} \tfrac{1}{2} |Y_t - \lambda|^2.$$

It is easy to verify that

$$I_n(\omega) = \sum_{t=1}^{n} \{\tfrac{1}{2} |Y_t - \lambda|^2 - \tfrac{1}{2} |Y_t - \lambda - \mathbf{x}_t^T(\omega)\bar{\boldsymbol{\beta}}_n(\omega)|^2\}, \tag{9}$$

where λ can be any constant, particularly $\lambda := \bar{\lambda}_n$. As we can see, the quantile periodograms simply replace the least-squares solution in (8) and (9) by a quantile regression solution. The quantile periodogram II also replaces the least-squares cost function by the corresponding quantile regression cost function.

Figure 1 demonstrates the ability of the quantile periodograms to detect hidden periodicity in the quantiles. Depicted in Figure 1 are the quantile periodograms, as functions of the normalized frequency $f := \omega/(2\pi)$ (in cycles per unit time), for a time series which is simulated according to (2) with $n = 200$ ($b_0 = 1$, $b_1 = 0.9$, $b_2 = 0$, and $\omega_0 = 2\pi \times 0.1$) and with $\{X_t\}$ being a second-order autoregressive, or AR(2), process (mean 0 and variance 1) satisfying

$$X_t = a_1 X_{t-1} + a_2 X_{t-2} + \xi_t \qquad (t = 1, \ldots, n), \tag{10}$$

where $a_1 := 2r\cos(\omega_c)$ and $a_2 := -r^2$ ($r = 0.6$ and $\omega_c = 2\pi \times 0.25$) and where $\{\xi_t\}$ is Gaussian white noise. The parameter λ in (3) and (5) is taken to be the sample α-quantile of the time series, which is also the choice in all other numerical examples. As we can see from Figure 1, the quantile periodograms successfully reveal the hidden periodicity as a large spike at frequency ω_0, whereas the ordinary and Laplace periodograms fail to do so. A theoretical explanation of this result will be given in the next section.

Like the ordinary periodogram, the quantile periodograms can serve as representations of serial dependence in the frequency domain for time series without hidden periodicity. As an example, Figure 2 depicts

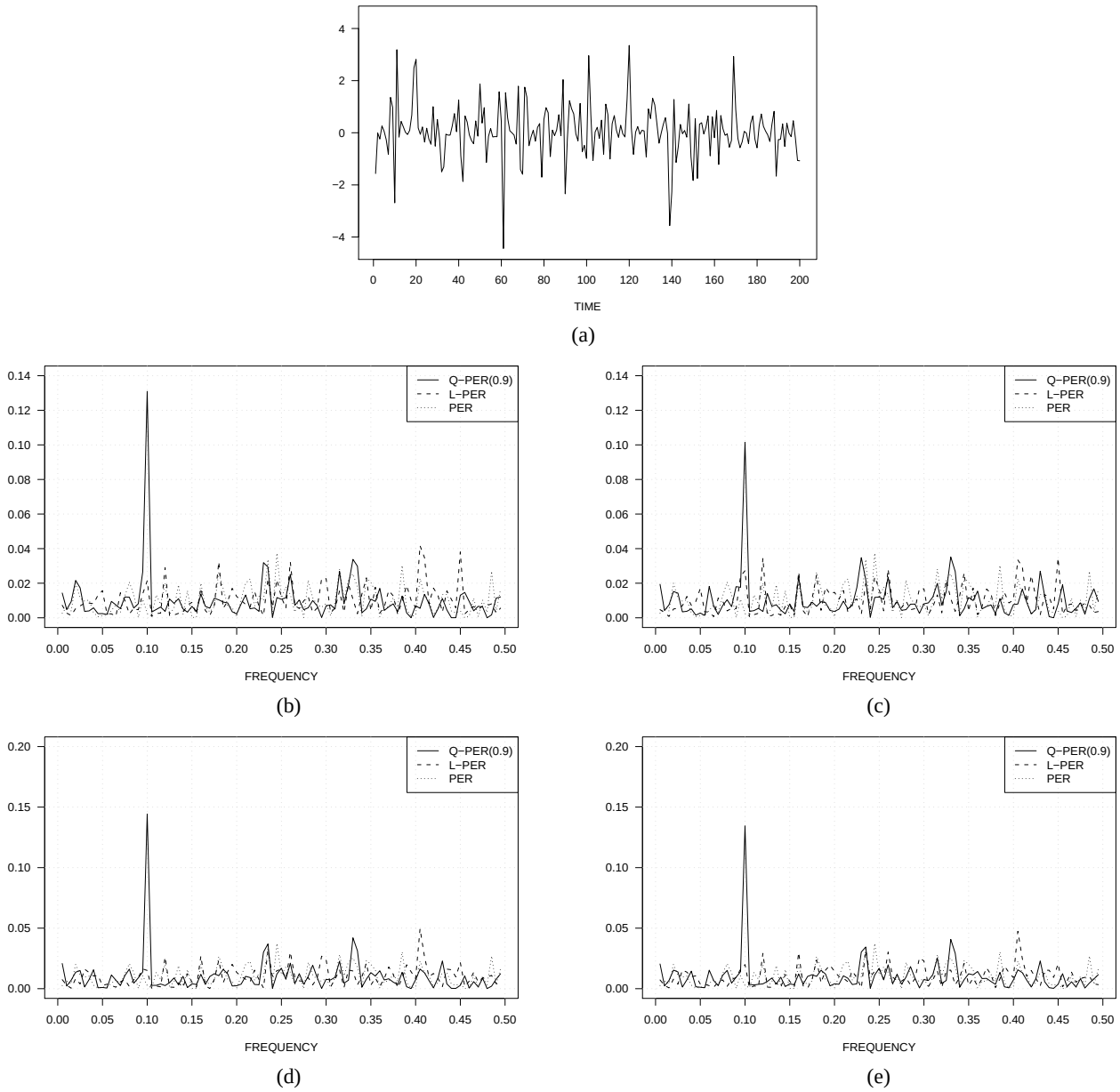

Figure 1: Quantile periodograms for a time series of the form (2). (a) The time series. (b) Quantile periodogram I defined by (3) and (4). (c) Quantile periodogram I defined by (6) and (4). (d) Quantile periodogram II defined by (3) and (5). (e) Quantile periodogram II defined by (6) and (7). —, quantile periodogram ($\alpha = 0.9$); - - -, Laplace periodogram; $\cdots$, ordinary periodogram. All periodograms are computed at the Fourier frequencies and standardized to sum up to unity for the convenience of display.

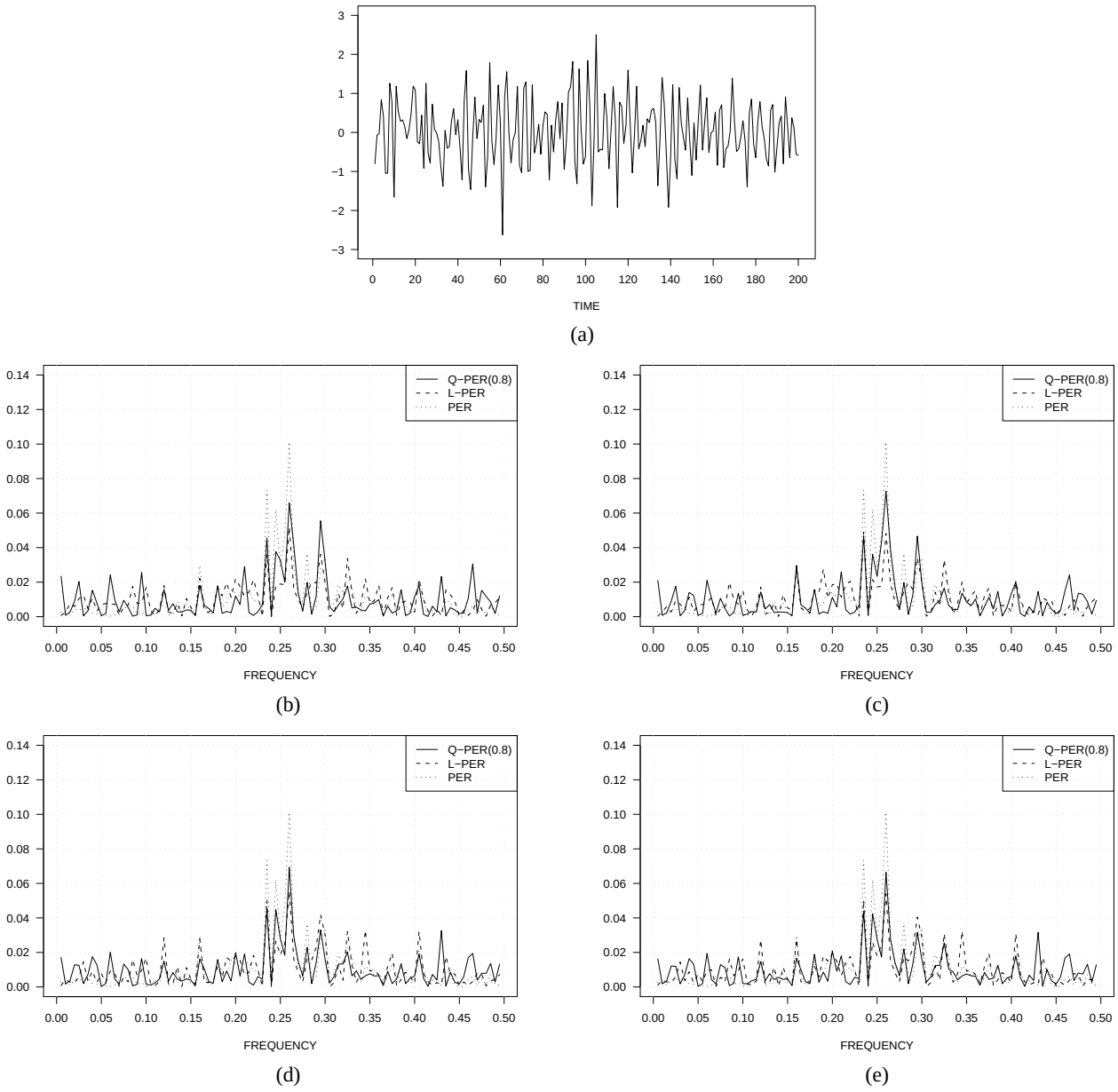

Figure 2: Quantile periodograms for a time series of the form (10). (a) The time series. (b) Quantile periodogram I defined by (3) and (4). (c) Quantile periodogram I defined by (6) and (4). (d) Quantile periodogram II defined by (3) and (5). (e) Quantile periodogram II defined by (6) and (7). —, quantile periodogram ($\alpha = 0.8$); - - -, Laplace periodogram; $\cdots$, ordinary periodogram. In (b) and (d), the parameter λ is taken to be the sample α-quantile of the time series. All periodograms are computed at the Fourier frequencies and standardized to sum up to unity for the convenience of display.

the quantile periodograms for a time series which is simulated according to (10) with $n = 200$ ($r = 0.8$ and $\omega_c = 2\pi \times 0.25$). The power spectrum of this process has a broad peak around ω_c. Figure 2 shows that the quantile periodograms behave similarly to the ordinary periodogram, exhibiting not only random variability across the frequency but a tendency of taking larger values around ω_c. It is not difficult to imagine that all these periodograms should yield bell-shaped curves when properly smoothed.

While the quantile periodograms can be examined at a specific quantile level α like the ordinary periodogram, they can also be analyzed as bivariate functions of α and ω to provide a much richer view of the time series. For illustration of such quantile-frequency analysis, consider the famous time series of yearly sunspot numbers which is shown in Figure 3(a). It is well known that the sunspot numbers have an 11-year cycle. This cycle manifests itself in the ordinary periodogram, shown in Figure 3(b), as the largest spectral peak at frequency $1/11 \approx 0.09$ (cycles per year). However, the 11-year cycle cannot be explained simply by a pure sinusoid because there are sizable secondary peaks on both sides of the main peak which together comprise a more complex phenomenon (Bloomfield 2000, p. 77). The quantile periodograms, shown in Figure 3(c) and (d) as bivariate functions of α and ω, reveal some additional complexity of the data: the secondary peaks round the main peak at the 11-year cycle are more pronounced at middle and upper quantiles but much weaker (if any) at lower quantiles. Such quantile-dependent spectral property of the sunspot numbers cannot be discerned from the ordinary periodogram.

3. Asymptotic Theory

It is well known that a smoothed ordinary periodogram constitutes an estimate of the power spectrum of the underlying random process that generates the time series. The Laplace periodograms are found to have a similar relationship with the so-called zero-crossing spectrum (Li 2008, 2012) which can be regarded as a frequency-domain representation of serial dependence for the underlying random process. A natural question to ask is what properties of the underlying random process do the quantile periodograms repre-

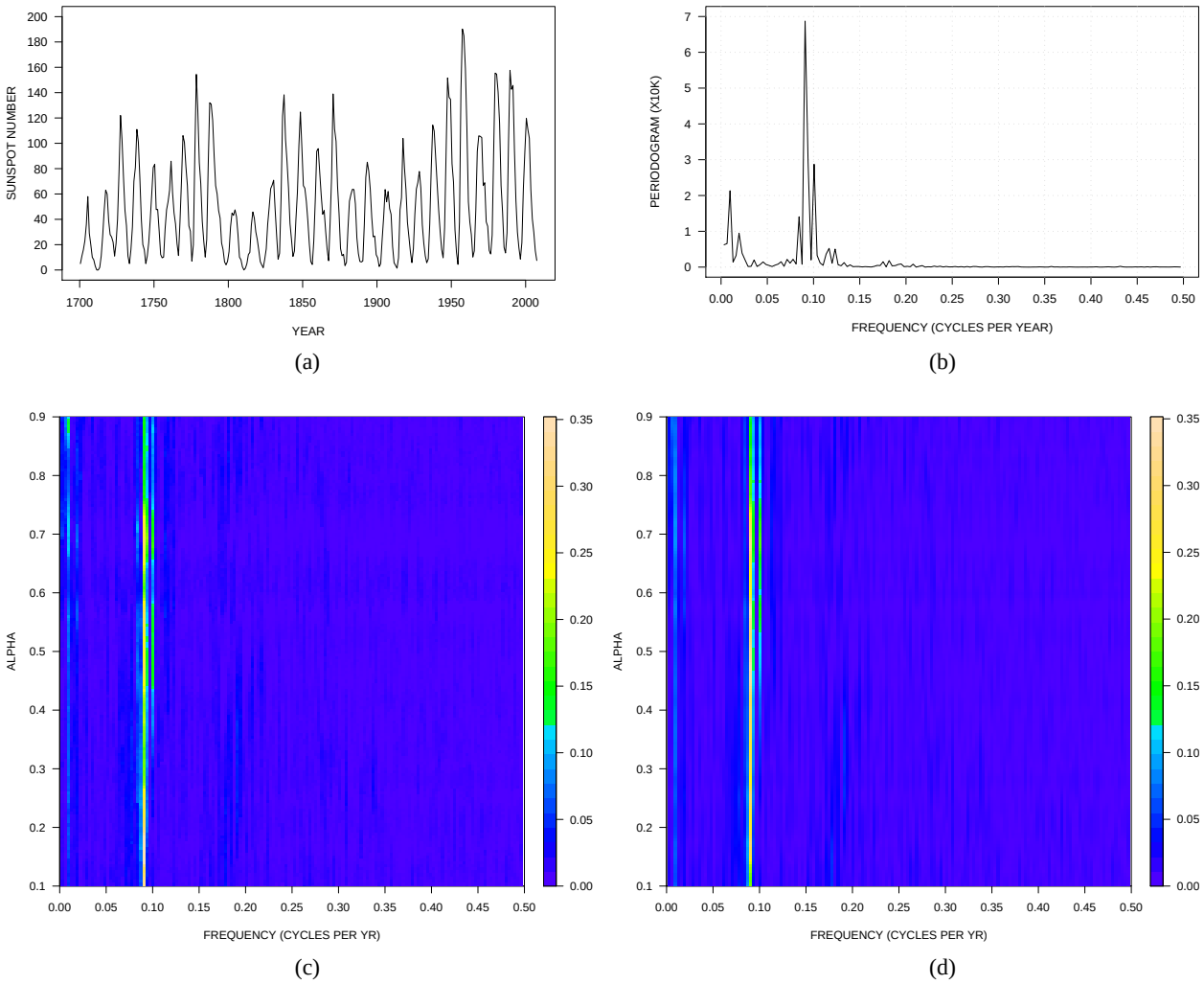

Figure 3: Quantile-frequency analysis. (a) Yearly sunspot numbers. (b) Ordinary periodogram. (c) Quantile periodogram I as bivariate function of the quantile level and frequency. (d) Quantile periodogram II bivariate function of the quantile level and frequency. The quantile periodograms are computed at the Fourier frequencies according to (4) and (7) and standardized to sum up to unity.

sent? While it is difficult to answer this question for finite sample sizes (or even to compute the mean and variance), the large sample asymptotic analysis in this section will reveal an association of the quantile periodograms with what we call the level-crossing spectrum which is analogous to the association of the Laplace periodograms with the zero-crossing spectrum. This result helps to explain the observations from Figure 2. The asymptotic analysis will also identify the impact of periodicity in the quantiles on the quantile periodograms. This result helps to explain the observations from Figure 1.

Assuming that $\{Y_t\}$ is a random process, let us consider the joint asymptotic distribution of the quantile periodogram ordinates computed at q distinct frequencies, denoted by $\omega_1, \ldots, \omega_q \in (0, \pi)$. Toward that end, let $F_t(u)$ and $F_{ts}(u,v)$ denote the univariate and bivariate marginal cumulative distribution functions of $\{Y_t\}$, and let the following conditions be satisfied for fixed α (and hence λ).

(C1) $f_t(u) := \dot{F}_t(u)$ exists for all u and $F_t(u+\lambda) - F_t(\lambda) = f_t(\lambda)u + O(u^{d+1})$ uniformly for $|u| \leq u_0$.

(C2) $F_t(\lambda) = \alpha$ and $f_t(\lambda) = \kappa > 0$ for all t.

(C3) $\{Y_t\}$ is stationary in λ-level crossings, i.e., $P\{(Y_t - \lambda)(Y_s - \lambda) < 0\} = \gamma_{t-s}$ for all t and s. We call γ_τ the lag-τ level-crossing rate (which depends on λ, of course).

(C4) $\{Y_t\}$ is an m-dependence process or a linear process of the form $\lambda + \sum_{l=-\infty}^{\infty} \varphi_l e_{t-l}$, where $\{e_t\}$ is an i.i.d. random sequence with $E(|e_t|) < \infty$ and $\{\varphi_l\}$ is an absolutely summable deterministic sequence such that $\sum_{|l|>n^r} \varphi_l = o(n^{-1})$ as $n \to \infty$ for some constant $r \in [0, 1/4)$. See Remark 1 in the appendix for relaxations of this technical assumption.

To better understand (C2) and (C3), consider the binary (0-1) level-crossing process $\{I(Y_t < \lambda)\}$. From (C2), it follows that

$$E\{I(Y_t < \lambda)\} = F_t(\lambda) = \alpha.$$

By (C2) and (C3), we can write

$$\begin{aligned}\gamma_{t-s} &= P(Y_t < \lambda, Y_s > \lambda) + P(Y_t > \lambda, Y_s < \lambda) \\ &= P(Y_t < \lambda) + P(Y_s < \lambda) - P(Y_t < \lambda, Y_s \le \lambda) - P(Y_t \le \lambda, Y_s < \lambda) \\ &= 2\{\alpha - F_{ts}(\lambda, \lambda)\},\end{aligned}$$

which, in turn, yields

$$\mathrm{Cov}\{I(Y_t < \lambda), I(Y_s < \lambda)\} = F_{ts}(\lambda, \lambda) - \alpha^2 = \alpha(1-\alpha) - (1/2)\gamma_{t-s}.$$

Therefore, under (C2) and (C3), the level-crossing process $\{I(Y_t < \lambda)\}$ is weakly stationary with mean α and autocovariance function $\alpha(1-\alpha) - (1/2)\gamma_\tau$.

The sequence $\{\gamma_\tau\}$ can be represented in the frequency domain by the Fourier transform

$$S(\omega) := \sum_{\tau=-\infty}^{\infty} \left\{1 - \frac{1}{2\alpha(1-\alpha)}\gamma_\tau\right\} \exp(i\omega\tau) = \sum_{\tau=-\infty}^{\infty} \left\{1 - \frac{1}{2\alpha(1-\alpha)}\gamma_\tau\right\} \cos(\omega\tau),$$

where the second expression is due to the symmetry of $\{\gamma_\tau\}$, i.e., $\gamma_{-\tau} = \gamma_\tau$ for all τ. We call $S(\omega)$ the level-crossing spectrum of $\{Y_t\}$. It is nothing but the ordinary power spectrum of the standardized (mean 0 and variance 1) level-crossing process $\{(I(Y_t < \lambda) - \alpha)/\sqrt{\alpha(1-\alpha)}\}$ whose autocovariance function equals $1 - \{2\alpha(1-\alpha)\}^{-1}\gamma_\tau$. Observe that an i.i.d. sequence with α-quantile λ is stationary in λ-level crossings with $\gamma_\tau = 2\alpha(1-\alpha)(1-\delta_\tau)$, in which case, $S(\omega) = 1$ for all ω. In general, the level-crossing spectrum serves as a scale-invariant frequency-domain representation of serial dependence from a different perspective than the ordinary autocorrelation spectrum (or the normalized power spectrum) defined as

$$R(\omega) := \sum_{\tau=-\infty}^{\infty} r_\tau \exp(i\omega\tau) = \sum_{\tau=-\infty}^{\infty} r_\tau \cos(\omega\tau),$$

where $\{r_\tau\}$ is the autocorrelation function of $\{Y_t\}$ under the assumption of stationarity in second moments.

Equipped with these concepts, the following theorem can be established. A proof is given in the appendix.

Theorem 1. *Let $\{Y_t\}$ satisfy the conditions (C1)–(C4). Let $Q_{n,\mathrm{I}}(\omega_j)$ and $Q_{n,\mathrm{II}}(\omega_j)$ $(j = 1,\ldots,q)$ be defined by (4) and (5) with $\hat{\boldsymbol{\beta}}_n(\omega)$ given by (3), or defined by (4) and (7) with $\hat{\lambda}_n(\omega)$ and $\hat{\boldsymbol{\beta}}_n(\omega)$ given by (6). Assume further that $S(\omega)$ is finite and bounded away from zero. Then, as $n \to \infty$,*

$$\{Q_{n,\mathrm{I}}(\omega_j)\} \overset{A}{\sim} \{(1/2)\eta_{\mathrm{I}}^2 S(\omega_j)\xi_{j,1}\}, \quad \{Q_{n,\mathrm{II}}(\omega_j)\} \overset{A}{\sim} \{(1/2)\eta_{\mathrm{II}}^2 S(\omega_j)\xi_{j,2}\},$$

where the symbol $\overset{A}{\sim}$ stands for "asymptotically distributed as," the sequences $\{\xi_{j,1}\}$ and $\{\xi_{j,2}\}$ comprise i.i.d. central chi-square random variables with 2 degrees of freedom, denoted as χ_2^2 or $\chi_2^2(0)$, and where $\eta_{\mathrm{I}}^2 := \alpha(1-\alpha)/\kappa^2$ and $\eta_{\mathrm{II}}^2 := \alpha(1-\alpha)/\kappa$ are scaling constants.

Theorem 1 shows that the quantile periodograms have scaled chi-square distributions with 2 degrees of freedom. This is similar to the behavior of the ordinary periodogram (Brockwell and Davis 1991, p. 347). The only difference is in the scaling function. For the ordinary periodogram, the scaling function is the power spectrum $p(\omega) := \sigma^2 R(\omega)$, where σ^2 is the variance and $R(\omega)$ is the autocorrelation spectrum of $\{Y_t\}$. According to Theorem 1, the scaling function associated with the quantile periodogram I is given by

$$q_{\mathrm{I}}(\omega) := \eta_{\mathrm{I}}^2 S(\omega), \tag{11}$$

and the scaling function associated with the quantile periodogram II takes the form

$$q_{\mathrm{II}}(\omega) := \eta_{\mathrm{II}}^2 S(\omega). \tag{12}$$

We call $q_{\mathrm{I}}(\omega)$ and $q_{\mathrm{II}}(\omega)$ the quantile spectrum of the first and second kind (or the quantile spectrum I and II), respectively. Both quantile spectra are proportional to the same level-crossing spectrum. The only difference is in the constant factors η_{I}^2 and η_{II}^2 which play a similar role to the variance σ^2 in the power spectrum. Observe that $\eta_{\mathrm{II}}^2 = \kappa\eta_{\mathrm{I}}^2$ and hence

$$q_{\mathrm{II}}(\omega) = \kappa q_{\mathrm{I}}(\omega). \tag{13}$$

This implies that the quantile spectrum II has a lower magnitude than the quantile spectrum I if $\kappa < 1$.

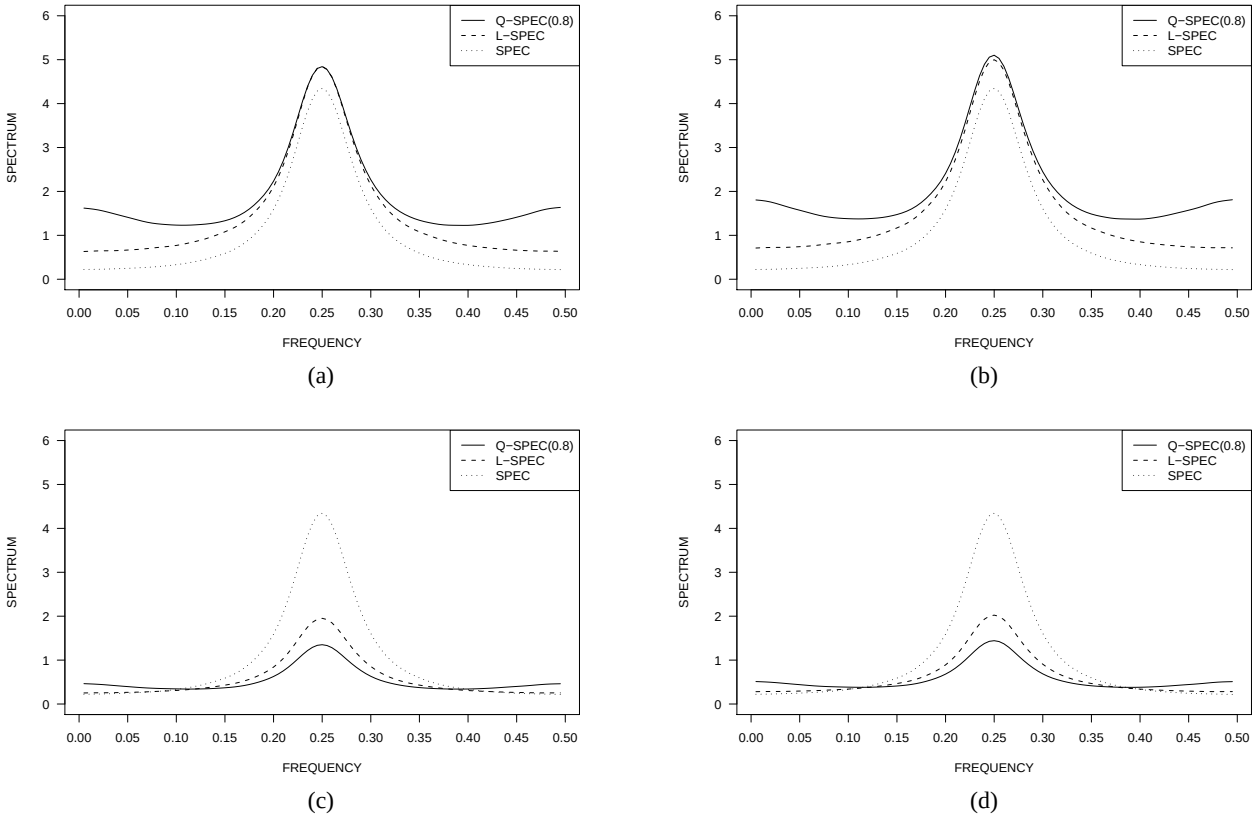

Figure 4: Ensemble mean of the quantile periodograms for an AR(2) process. (a) Mean quantile periodogram I defined by (3) and (4). (b) Mean quantile periodogram I defined by (6) and (4). (c) Mean quantile periodogram II defined by (3) and (5). (d) Mean quantile periodogram II defined by (6) and (7). —, mean quantile periodogram ($\alpha = 0.8$); - - -, mean Laplace periodogram; $\cdots$, mean ordinary periodogram. Results are based on 5000 Monte Carlo runs with $n = 200$.

As an example, Figure 4 depicts the ensemble mean of the quantile periodograms together with the ensemble mean of the ordinary and Laplace periodograms, all obtained from 5000 independent realizations of the AR(2) process in (10) with $n = 200$ ($r = 0.8$ and $\omega_c = 2\pi \times 0.25$). Although not exactly the quantile spectra as defined, these finite-sample ensemble means do exhibit a similar bell-shaped pattern expected for the power spectrum of the AR(2) process. Note that the mean quantile periodogram II has a lower magnitude than the mean quantile periodogram I due to a different scaling factor. According to (13), one can make the quantile periodogram II comparable in magnitude to the quantile periodogram I by multiplying the former with an estimate of the quantity $1/\kappa$ which is known as the sparsity (reciprocal of the density). See Koenker (2005, p. 139) for details on sparsity estimation.

The autocorrelation function and its Fourier transform are the traditional scale-invariant representations of serial dependence. In the Gaussian case, a simple relationship exists between the level-crossing rates and the autocorrelation coefficients. This relationship links the level-crossing spectrum directly to the autocorrelation spectrum as their respective Fourier transforms. Indeed, under (C2) and (C3), we can write

$$\gamma_\tau = 2(\alpha - p_\tau), \tag{14}$$

where $p_\tau := P(Y_{t+\tau} \leq \lambda, Y_t \leq \lambda)$ is a noncentered orthant probability. If $\{Y_t\}$ is a stationary Gaussian process with mean zero, variance σ^2, and autocorrelation function $\{r_\tau\}$, then it can be shown (see the appendix) that

$$p_\tau = \int_{-\infty}^{\lambda/\sigma} \Phi\left(\frac{\lambda/\sigma - r_\tau x}{\sqrt{1-r_\tau^2}}\right)\phi(x)\,dx, \tag{15}$$

where $\phi(x)$ and $\Phi(x)$ denote the probability density function and the cumulative distribution function of the standard normal random variable. The combination of (15) with (14) shows that γ_τ is a direct yet nontrivial transformation of r_τ. Note that p_τ is scale-invariant because both λ/σ and r_τ are scale-invariant.

Owing to their association with the level-crossing spectrum, the quantile periodograms are also invariant to nonlinear distortion of the data in the sense that any nonlinear memoryless transform of Y_t only affects the scaling constant in the asymptotic distribution of the quantile periodograms provided that the nonlinearity

Table 1: Periodogram Smoothing: Variance-Bias Tradeoff in Mean-Square Error*

	Ordinary Periodogam			Laplace Periodogram			Quantile Periodogram†		
df	MSE	$BIAS^2$	VAR	MSE	$BIAS^2$	VAR	MSE	$BIAS^2$	VAR
30	0.537	0.000	0.537	1.165	0.000	1.165	1.639	0.000	1.639
25	0.429	0.001	0.438	1.014	0.001	1.013	1.440	0.001	1.439
10	0.199	0.039	0.160	0.614	0.038	0.575	0.905	0.037	0.868
5	0.378	0.306	0.072	0.716	0.314	0.402	0.965	0.309	0.656

$*$ Results are based on 5000 Monte Carlo runs. † Quantile periodogram is defined by (6) and (4) with $\alpha = 0.8$.

preserves the specified quantile. The ordinary periodogram does not have this advantage, as nonlinearity will deform the entire power spectrum in a nontrivial way (Wise, Traganitis, and Thomas 1977).

Theorem 1 suggests that the quantile spectra, defined by (11) and (12), can be estimated nonparametrically by smoothing the quantile periodogram ordinates at the Fourier frequencies in the same way as the power spectrum can be estimated by smoothing the ordinary periodogram ordinates. As with the smoothed ordinary periodogram, there is a tradeoff between bias and variance in the mean-square error (MSE) of a smoothed quantile periodogram. To demonstrate the tradeoff, we resort to a Monte Carlo simulation, as the mean and variance of the quantile periodograms cannot be evaluated analytically.

Table 1 contains the MSE of the smoothed quantile periodogram I for estimating the quantile spectrum I of the AR(2) process in (10) with $n = 200$ ($r = 0.8$ and $\omega_c = 2\pi \times 0.25$). The smoothed quantile periodogram is obtained by the standard technique of smoothing splines which is implemented in R as `smooth.spline`. The amount of smoothing is controlled by a parameter called the degree of freedom (df): the smaller the df, the greater the amount of smoothing. For comparison, the ordinary and Laplace periodograms are smoothed in the same way. As can be seen from Table 1, the bias of the smoothed quantile periodogram increases with the decrease of the df whereas the variance decreases with it, so a minimum MSE can be achieved by

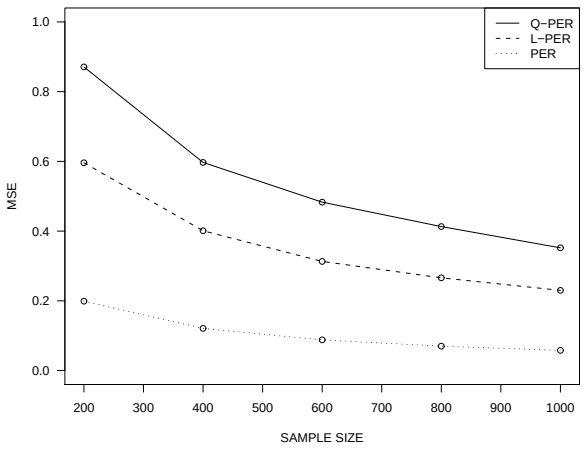

Figure 5: Mean-square error of smoothed periodograms for an AR(2) process. —, quantile periodogram defined by (3) and (4) ($\alpha = 0.8$); - - -, Laplace periodogram; $\cdots$, ordinary periodogram. Results are based on 5000 Monte Carlo runs.

balancing the bias and the variance. This is the same behavior of the smoothed ordinary periodogram.

It is well known that the power spectrum can be estimated consistently by a properly smoothed ordinary periodogram (Brockwell and Davis 1991, pp. 350–353). The lack of analytical expressions for the mean and variance of the quantile periodograms makes it difficult to conduct a similar investigation for the smoothed quantile periodograms as estimators of the quantile spectra. However, our simulation studies do confirm that the MSE decreases with the increase of n. As an example, Figure 5 depicts the MSE of the smoothed quantile periodogram as a function of n which takes on values from 200 to 1000. For comparison, the MSE of the smoothed ordinary periodogram is also depicted. In both cases, the smoothing parameter df is selected for each sample size to minimize the MSE. Figure 5 shows that the MSE of the smoothed quantile periodogram indeed decreases with the increase of n in a way similar to the MSE of the smoothed ordinary periodogram.

Theorem 1 also suggests that an approximate confidence interval for the quantile spectra can be constructed by using the well-known χ^2 approximation technique (Brockwell and Davis 1991, p. 362). To be

more specific, consider the smoothed quantile periodogram I of the form $\hat{q}_{\mathrm{I}}(\omega_j) := \sum_{|k|\le m} W_{nk} Q_{n,\mathrm{I}}(\omega_j + \omega_k)$, where the $W_{nk} \ge 0$ are suitable weights that sum up to unity and the ω_j denote the Fourier frequencies. The idea is to use a scaled chi-square distribution, $\mu\chi^2_\nu$, to approximate the distribution of $\hat{q}_{\mathrm{I}}(\omega_j)$, where $\mu > 0$ and $\nu > 0$ are chosen so that the mean and variance of $\mu\chi^2_\nu$ are equal to $q_{\mathrm{I}}(\omega_j)$ and $(\sum_{|k|\le m} W^2_{nk}) q^2_{\mathrm{I}}(\omega_j)$. This leads to $\mu = (\sum_{|k|\le m} W^2_{nk}) q_{\mathrm{I}}(\omega_j)/2$ and $\nu = 2/(\sum_{|k|\le m} W^2_{nk})$. Hence, an approximate 95% confidence interval for $q_{\mathrm{I}}(\omega_j)$ takes the form $(\nu\hat{q}_{\mathrm{I}}(\omega_j)/\chi^2_{\nu,0.975}, \nu\hat{q}_{\mathrm{I}}(\omega_j)/\chi^2_{\nu,0.025})$.

To help understand the ability of the quantile periodograms to detect hidden periodicity in the quantiles, let us assume that the α-quantile of Y_t takes the form

$$\lambda_t = \lambda + \mathbf{x}_t^T(\omega_0)\boldsymbol{\beta}_0, \tag{16}$$

where $\omega_0 \in (0,\pi)$ and $\boldsymbol{\beta}_0 \neq \mathbf{0}$. As mentioned earlier, if $\{Y_t\}$ is given by (2) with X_t having a constant α-quantile c for all t, then $\lambda_t = ca_t$ can be expressed as (16). Under the assumption (16), the following result can be obtained. A proof is given in the appendix.

Theorem 2. *Let $\{Y_t\}$ satisfy (C1)–(C4) with λ replaced by λ_t of the form (16). Assume further that $0 < S(\omega_0) < \infty$. Then, as $n \to \infty$,*

$$Q_{n,\mathrm{I}}(\omega_0) \overset{A}{\sim} (1/2)\eta^2_{\mathrm{I}} S(\omega_0)\chi^2_2(\theta_n), \quad Q_{n,\mathrm{II}}(\omega_0) \overset{A}{\sim} \Delta_n + (1/2)\eta^2_{\mathrm{II}} S(\omega_0)\chi^2_2,$$

where $\theta_n := (1/2)n\|\boldsymbol{\beta}_0\|_2^2/(\eta^2_{\mathrm{I}} S(\omega_0))$, $\Delta_n := \sum_{t=1}^n \{\rho_\alpha(Y_t - \lambda) - \rho_\alpha(Y_t - \lambda - \mathbf{x}_t^T(\omega_0)\boldsymbol{\beta}_0)\}$ if $Q_{n,\mathrm{II}}(\omega)$ is defined by (3) and (5), and $\Delta_n := \sum_{t=1}^n \{\rho_\alpha(Y_t - \hat{\lambda}_n) - \rho_\alpha(Y_t - \tilde{\lambda}_n - \mathbf{x}_t^T(\omega_0)\boldsymbol{\beta}_0)\}$ if $Q_{n,\mathrm{II}}(\omega)$ is defined by (6) and (7), in which case, $\hat{\lambda}_n$ is defined by (1) and $\tilde{\lambda}_n := \arg\min_\lambda \sum_{t=1}^n \rho_\alpha(Y_t - \lambda - \mathbf{x}_t^T(\omega_0)\boldsymbol{\beta}_0)$.

By comparing Theorem 2 with Theorem 1, we can see that the periodicity is manifested in the quantile periodogram I as the noncentrality parameter θ_n in a noncentral chi-square distribution, and that it is manifested in the quantile periodogram II as the additive term Δ_n to a central chi-square distribution. Both θ_n and Δ_n measure the strength of the periodicity: θ_n focuses on the amplitude of the periodicity directly while

Δ_n focuses on its net contribution to the cost function. These manifestations of the periodicity explain why a large spike tends to occur in the quantile periodograms at frequency ω_0.

Figure 6 demonstrates the effect of periodicity on the quantile periodograms by depicting the ensemble mean of the quantile periodograms for time series generated according to (2) with $n = 200$ ($b_0 = 1$, $b_1 = 0.6$, $b_2 = 0$, $\omega_0 = 2\pi \times 0.1$, $r = 0.6$, and $\omega_c = 2\pi \times 0.25$). The corresponding ensemble means of the ordinary and Laplace periodograms are also shown. As we can see, the mean quantile periodograms exhibit a large spike at ω_0, which is consistent with the asymptotic results in Theorem 2. In contrast, the spike is completely missing in the ensemble mean of the ordinary and Laplace periodograms, which can be explained by the fact that the mean and the median of the process in (2) are both equal to zero for all t.

Note that Theorem 2 concerns only about the distribution at the signal frequency ω_0. While the distribution at other frequencies can be derived similarly with the help of the Quantile Regression Lemma in the appendix, as done in Li (2008) for the Laplace periodogram, a more detailed analysis will be given elsewhere. We simply point out that spectral leak, which has been observed for the Laplace periodogram, is also possible for the quantile periodograms. As a result, small spikes may occur at some other frequencies (e.g., the integral multiples of ω_0), especially when the periodicity is strong, so that the distribution at these frequencies may not be the same as the one suggested by Theorem 1.

Based on the ordinary periodogram, the Kolmogorov-Smirnov test and Fisher's test (Brockwell and Davis 1991, pp. 339–314) are standard procedures for detection of periodicity in the mean of a random process. These procedures are readily applicable to the quantile periodograms for detection of periodicity in the quantiles. As an example, consider the statistic

$$g := \frac{\max\{I_n(\omega_k)\}}{\sum I_n(\omega_k)},$$

where the max and the sum are taken over the set of Fourier frequencies ω_k in the interval $(0, \pi)$. Fisher's test declares the presence of hidden periodicity if g is sufficiently large. By replacing the ordinary periodogram with a quantile periodogram, the g statistic can be used to test for hidden periodicity in the quantiles.

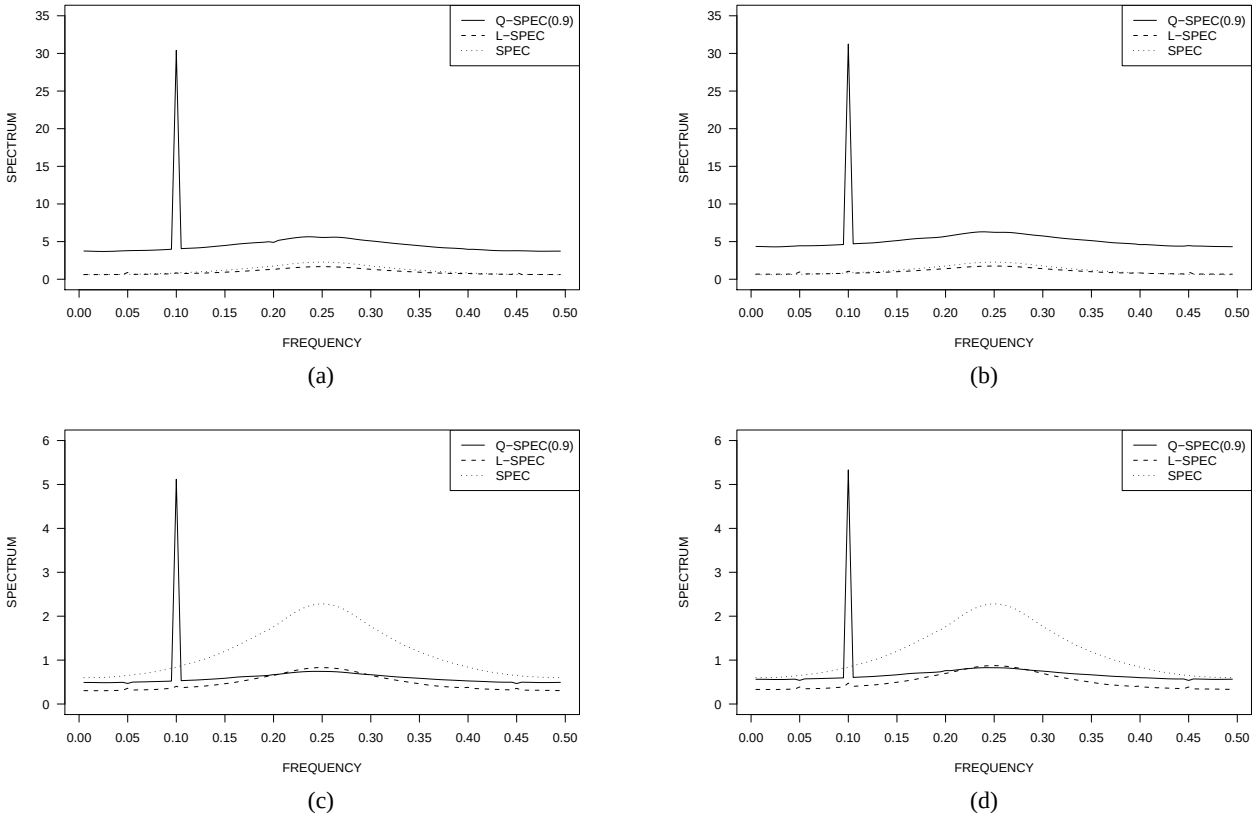

Figure 6: Ensemble mean of the quantile periodograms for time series of the form (2). (a) Mean quantile periodogram I defined by (3) and (4). (b) Mean quantile periodogram I defined by (6) and (4). (c) Mean quantile periodogram II defined by (3) and (5). (d) Mean quantile periodogram II defined by (6) and (7). —, mean quantile periodogram ($\alpha = 0.9$); - - -, mean Laplace periodogram; $\cdots$, mean ordinary periodogram. Results are based on 5000 Monte Carlo runs with $n = 200$.

Table 2: Detection Power of Fisher's Test*

Probability of	Quantile Periodogam†			Laplace	Ordinary	Level Crossing
False Alarm	$\alpha = 0.9$	$\alpha = 0.8$	$\alpha = 0.7$	Periodogram	Periodogram	$\alpha = 0.9$
0.01	0.83	0.58	0.16	0.01	0.00	0.55
0.05	0.95	0.82	0.38	0.05	0.02	0.80
0.10	0.98	0.91	0.50	0.10	0.04	0.87

$*$ Results are based on 5000 Monte Carlo runs. † Quantile periodogram is defined by (6) and (7).

The power of this test is demonstrated by Table 2, where the probability of detection is computed on the basis of a Monte Carlo simulation for time series of the form (2) with $n = 200$ ($b_0 = 1$, $b_1 = 0.8$, $b_2 = 0$, $\omega_0 = 2\pi \times 0.1$, $r = 0.6$, and $\omega_c = 2\pi \times 0.25$). As can be seen, at significance level 0.05, for example, the quantile periodogram with $\alpha = 0.9$ has a 95% chance of detecting the periodicity, whereas the probability of detection by the ordinary periodogram and the Laplace periodogram is merely 2% and 5%, respectively. Note that the detection power does depend on α, albeit not super-sensitive to the choice. For example, with $\alpha = 0.8$, the chance of detection reduces to 82%. Therefore, to maximize the detection power, a proper selection of α is necessary. If multiple values of α are experimented in cases where a suitable value cannot be determined in advance, one has to deal with the possibility of false discovery due to multiple testing.

Given the fact that the quantile periodograms are related to the level-crossing spectrum, why not simply consider the ordinary periodogram of the level-crossing process $\{I(Y_t < \lambda)\}$? This method has an immediate appeal of computational simplicity, as the ordinary periodogram can be computed by the fast Fourier transform. But, the loss of information in transforming a real-valued time series into a binary-valued level-crossing process may cause degradation of statistical efficiency. This is demonstrated by the example in Table 2 (the column labeled "Level Crossing"). As compared to the quantile periodogram with $\alpha = 0.9$, the ordinary periodogram of the corresponding level-crossing process loses the detection power by 11–28% in

absolute terms, depending on the false-alarm probability.

In closing, we remark that the asymptotic analysis in this section can be extended in multiple directions. For example, one can derive the joint asymptotic distribution of the quantile periodograms at multiple quantile levels in order to better understand the behavior of the quantile periodograms for quantile-frequency analysis. One can also investigate the limiting properties of the quantile periodograms at extremely high quantiles relative to the sample size. This would cast some light on the capability of the quantile periodograms for analyzing the dependence of extreme values in time-series data. It is also possible to extend the quantile periodograms to multi-dimensional data. Finally, one can easily generalize the quantile periodogram I along the lines of Li (2010) for spectral coherence analysis of multiple time series.

Appendix: Lemma and Proofs

1. Quantile Regression Lemma

To facilitate the proof of the main theorems, consider a more general quantile regression problem. For each $j = 1, \ldots, q$, let $\{\mathbf{x}_{jt}\}$ be a bounded sequence of deterministic vectors in $\mathbb{R}^p$ and define

$$\hat{\boldsymbol{\beta}}_{jn} := \arg\min_{\boldsymbol{\beta} \in \mathbb{R}^p} \sum_{t=1}^{n} \rho_\alpha(Y_t - \mathbf{x}_{jt}^T \boldsymbol{\beta}).$$

To develop an asymptotic theory for this problem, let Y_t take the form

$$Y_t := c_t + \varepsilon_t \quad (t = 1, \ldots, n),$$

where $\{c_t\}$ is a deterministic sequence and $\{\varepsilon_t\}$ is a random sequence. For any constant vector $\boldsymbol{\beta}_j \in \mathbb{R}^p$, define $w_{jt} := \mathbf{x}_{jt}^T \boldsymbol{\beta}_j - c_t$. Let $G_t(u)$ and $G_{ts}(u,v)$ denote the univariate and bivariate marginal cumulative distribution functions of $\{\varepsilon_t\}$, i.e., $\varepsilon_t \sim G_t(u)$ and $(\varepsilon_t, \varepsilon_s) \sim G_{ts}(u,v)$. With this notation, let the following assumptions be satisfied.

(A1) The derivative of $G_t(u)$ with respect to u, denoted as $g_t(u) := \dot{G}_t(u)$, exists for all u and satisfies $g_t(w_{jt}) = O(1)$ uniformly.

(A2) $G_t(u+w_{jt}) - G_t(w_{jt}) = g_t(w_{jt})u + O(u^{d+1})$ uniformly for $|u| \le u_0$, where $d > 0$ and $u_0 > 0$ are some constants.

(A3) $\mathbf{\Lambda}_{jn} := n^{-1}\sum_{t=1}^{n} g_t(w_{jt})\mathbf{x}_{jt}\mathbf{x}_{jt}^T \ge \mathbf{\Lambda}_0$ for all j and for large n, where $\mathbf{\Lambda}_0$ is a positive definite matrix.

(A4) $\mathbf{C}_{jkn} := n^{-1}\sum_{t=1}^{n}\sum_{s=1}^{n} r_{ts}(w_{jt}, w_{ks})\mathbf{x}_{jt}\mathbf{x}_{ks}^T \ge \mathbf{C}_0$ for all j, k, and for large n, where $\mathbf{C}_0$ is a positive definite matrix and $r_{ts}(u,v) := G_{ts}(u,v) - G_t(u)G_s(v)$.

(A5) $\{\varepsilon_t\}$ is an m-dependence process or a linear process of the form $\varepsilon_t := \sum_{l=-\infty}^{\infty}\varphi_l e_{t-l}$, where $\{e_t\}$ is an i.i.d. random sequence with $E(|e_t|) < \infty$ and $\{\varphi_l\}$ is an absolutely summable deterministic sequence such that $\sum_{|l|>n^r}\varphi_l = o(n^{-1})$ for some constant $r \in [0, 1/4)$. See Remark 1 for relaxations of this technical assumption.

Then, the following result can be obtained.

Lemma (Quantile Regression Lemma). *If (A1)–(A5) are satisfied, then, as $n \to \infty$,*

$$\sqrt{n}\,\mathrm{vec}[\hat{\boldsymbol{\beta}}_{jn} - \boldsymbol{\beta}_j]_{j=1}^{q} \overset{A}{\sim} N(\boldsymbol{\mu}_n, \mathbf{\Sigma}_n),$$

where $\boldsymbol{\mu}_n := \mathrm{vec}[\mathbf{\Lambda}_{jn}^{-1}\mathbf{h}_{jn}]_{j=1}^{q}$, $\mathbf{\Sigma}_n := [\mathbf{\Lambda}_{jn}^{-1}\mathbf{C}_{jkn}\mathbf{\Lambda}_{kn}^{-1}]_{j,k=1}^{q}$, *and* $\mathbf{h}_{jn} := n^{-1/2}\sum_{t=1}^{n}\{\alpha - G_t(w_{jt})\}\mathbf{x}_{jt}$. *Moreover, let* $\psi_\alpha(u) := \alpha - I(u<0)$ *and* $\boldsymbol{\zeta}_{jn} := n^{-1/2}\sum_{t=1}^{n}\psi_\alpha(Y_t - \mathbf{x}_{jt}^T\boldsymbol{\beta}_j)\mathbf{x}_{jt}$. *Then, as $n \to \infty$,*

$$\sum_{t=1}^{n}\rho_\alpha(Y_t - \mathbf{x}_{jt}^T\hat{\boldsymbol{\beta}}_{jn}) = \sum_{t=1}^{n}\rho_\alpha(Y_t - \mathbf{x}_{jt}^T\boldsymbol{\beta}_j) - \frac{1}{2}\boldsymbol{\zeta}_{jn}^T\mathbf{\Lambda}_{jn}^{-1}\boldsymbol{\zeta}_{jn} + o_P(1),$$

and the $\boldsymbol{\zeta}_{jn}$ *are asymptotically jointly normal such that* $\mathrm{vec}[\boldsymbol{\zeta}_{jn}]_{j=1}^{q} \overset{A}{\sim} N(\mathrm{vec}[\mathbf{h}_{jn}]_{j=1}^{q}, [\mathbf{C}_{jkn}]_{j,k=1}^{q})$.

PROOF. The proof follows the lines of Knight (1998), Koenker (2005), and Li (2008). First, consider the case of $q = 1$ for which we drop the subscript j in the notation for simplicity. For any $\boldsymbol{\delta} \in \mathbb{R}^p$, let

$$Z_n(\boldsymbol{\delta}) := \sum_{t=1}^{n}\{\rho_\alpha(U_t - v_{nt}(\boldsymbol{\delta})) - \rho_\alpha(U_t)\}, \tag{17}$$

where $U_t := Y_t - \mathbf{x}_t^T\boldsymbol{\beta} = \varepsilon_t - w_t$ and $v_{nt}(\boldsymbol{\delta}) := n^{-1/2}\mathbf{x}_t^T\boldsymbol{\delta}$. The objective is to show that for each fixed $\boldsymbol{\delta} \in \mathbb{R}^p$,

$$Z_n(\boldsymbol{\delta}) = \tilde{Z}_n(\boldsymbol{\delta}) + o_P(1), \tag{18}$$

where $\tilde{Z}_n(\boldsymbol{\delta}) := -\boldsymbol{\delta}^T\boldsymbol{\zeta}_n + (1/2)\boldsymbol{\delta}^T\boldsymbol{\Lambda}_n\boldsymbol{\delta}$ and $\boldsymbol{\zeta}_n \overset{A}{\sim} N(\mathbf{h}_n, \mathbf{C}_n)$. Because $Z_n(\boldsymbol{\delta})$ and $\tilde{Z}_n(\boldsymbol{\delta})$ are convex functions of $\boldsymbol{\delta}$, an application of the Convexity Lemma in Pollard (1991) would strengthen (18) to uniformity in $\boldsymbol{\delta} \in \Delta$ for any given compact set $\Delta \in \mathbb{R}^p$. Then, by following the last part in the proof of Theorem 1 in Pollard (1991), we would be able to show that the minimizer of $Z_n(\boldsymbol{\delta})$, which we denote as $\hat{\boldsymbol{\delta}}_n$, is $o_P(1)$ away from the minimizer of $\tilde{Z}_n(\boldsymbol{\delta})$, which equals $\tilde{\boldsymbol{\delta}}_n := \boldsymbol{\Lambda}_n^{-1}\boldsymbol{\zeta}_n$. This result would lead to

$$\sqrt{n}(\hat{\boldsymbol{\beta}}_n - \boldsymbol{\beta}) = \hat{\boldsymbol{\delta}}_n = \tilde{\boldsymbol{\delta}}_n + o_P(1) \overset{A}{\sim} N(\boldsymbol{\Lambda}_n^{-1}\mathbf{h}_n, \boldsymbol{\Lambda}_n^{-1}\mathbf{C}_n\boldsymbol{\Lambda}_n^{-1}),$$

which is the first assertion. The second assertion would follow immediately from the fact that

$$Z_n(\hat{\boldsymbol{\delta}}_n) = \tilde{Z}_n(\tilde{\boldsymbol{\delta}}) + o_P(1), \quad \tilde{Z}_n(\tilde{\boldsymbol{\delta}}_n) = -\frac{1}{2}\boldsymbol{\zeta}_n^T\boldsymbol{\Lambda}_n^{-1}\boldsymbol{\zeta}_n.$$

Therefore, it suffices to establish (18) for each fixed $\boldsymbol{\delta} \in \mathbb{R}^p$.

Toward that end, observe that $\rho_\alpha(u) = (1/2)|u| + (\alpha - 1/2)u$. Combining this result with Knight's identity (Knight 1998)

$$|u-v| - |v| = -v\{1 - 2I(u < 0)\} + 2\int_0^v \{I(u \le x) - I(u \le 0)\}\, dx$$

leads to

$$\rho_\alpha(u-v) - \rho_\alpha(u) = -v\psi_\alpha(u) + \int_0^v \phi(u,x)\, dx,$$

where $\psi_\alpha(u) := \alpha - I(u < 0)$ is the derivative of $\rho_\alpha(u)$ and $\phi(u,x) := I(u \le x) - I(u \le 0)$ is a function which does not depend on α. Therefore, we can decompose $Z_n(\boldsymbol{\delta})$, defined by (17), as

$$Z_n(\boldsymbol{\delta}) = -\boldsymbol{\delta}^T\boldsymbol{\zeta}_n + R_n(\boldsymbol{\delta}),$$

where

$$\boldsymbol{\zeta}_n := n^{-1/2}\sum_{t=1}^n \psi_\alpha(U_t)\mathbf{x}_t, \quad R_n(\boldsymbol{\delta}) := \sum_{t=1}^n \int_0^{v_{nt}(\boldsymbol{\delta})} \phi(U_t, x)\, dx.$$

Because $R_n(\boldsymbol{\delta})$ does not depend on α, citing the result in Li (2008) for the case of $\alpha = 1/2$ under (A1)–(A3) gives

$$R_n(\boldsymbol{\delta}) = \frac{1}{2}\boldsymbol{\delta}^T \boldsymbol{\Lambda}_n \boldsymbol{\delta} + o_P(1)$$

for each fixed $\boldsymbol{\delta}$. Therefore, it remains to show that $\boldsymbol{\zeta}_n$ has a central limit theorem.

To prove this assertion under (A4) and (A5), assume first that $\{\varepsilon_t\}$ is an m-dependent process. In this case, the process $\{\psi_\alpha(U_t)\mathbf{x}_t^T\boldsymbol{\delta}\}$ is uniformly bounded and m-dependent. Moreover, straightforward calculation yields

$$E\{\psi_\alpha(U_t)\} = \alpha - F_t(w_t), \quad \text{Cov}\{\psi_\alpha(U_t), \psi_\alpha(U_s)\} = r_{ts}(w_t, w_s).$$

Therefore, we have $E(\boldsymbol{\delta}^T\boldsymbol{\zeta}_n) = \boldsymbol{\delta}^T\mathbf{h}_n$ and $\text{Var}(\boldsymbol{\delta}^T\boldsymbol{\zeta}_n) = \boldsymbol{\delta}^T\mathbf{C}_n\boldsymbol{\delta}$. By the central limit theorem for uniformly bounded m-dependent processes (Chung 2001, Theorem 7.3.1), we obtain $\boldsymbol{\delta}^T\boldsymbol{\zeta}_n \overset{A}{\sim} N(\boldsymbol{\delta}^T\mathbf{h}_n, \boldsymbol{\delta}^T\mathbf{C}_n\boldsymbol{\delta})$. Because this result holds for any $\boldsymbol{\delta}$, it follows from the Wald device that $\boldsymbol{\zeta}_n \overset{A}{\sim} N(\mathbf{h}_n, \mathbf{C}_n)$. If $\{\varepsilon_t\}$ is a linear process that satisfies (A5), then the central limit theorem can be established by following the proof of the Corollary in the complete version of Li (2008) based on an extension of Theorem 7.3.1 in Chung (2001) for uniformly bounded m-dependent processes with $m = O(n^r)$.

For the general case of $q > 1$, let $\boldsymbol{\delta} := \text{vec}[\boldsymbol{\delta}_j]_{j=1}^q := [\boldsymbol{\delta}_1^T, \ldots, \boldsymbol{\delta}_q^T]^T \in \mathbb{R}^{pq}$ and consider

$$Z_n(\boldsymbol{\delta}) := \sum_{j=1}^{q} Z_{jn}(\boldsymbol{\delta}_j),$$

where $Z_{nj}(\boldsymbol{\delta}_j)$ takes the form (17) except that $\mathbf{x}_t^T\boldsymbol{\delta}$ is replaced by $\mathbf{x}_{jt}^T\boldsymbol{\delta}_j$. By a similar argument, it can be shown that the minimizer of $Z_n(\boldsymbol{\delta})$, which can be expressed as $\hat{\boldsymbol{\delta}}_n := \text{vec}[\hat{\boldsymbol{\delta}}_{jn}]_{j=1}^q$, is $o_P(1)$ away from $\tilde{\boldsymbol{\delta}}_n := \text{vec}[\tilde{\boldsymbol{\delta}}_{jn}]_{j=1}^q$, where $\hat{\boldsymbol{\delta}}_{jn}$ is the minimizer of $Z_{jn}(\boldsymbol{\delta}_j)$ and $\tilde{\boldsymbol{\delta}}_{jn} := \boldsymbol{\Lambda}_{jn}^{-1}\boldsymbol{\zeta}_{jn}$ is the minimizer of $\tilde{Z}_{jn}(\boldsymbol{\delta}_j) := -\boldsymbol{\delta}_j^T\boldsymbol{\zeta}_{jn} + (1/2)\boldsymbol{\delta}_j^T\boldsymbol{\Lambda}_{jn}\boldsymbol{\delta}_j$. In these expressions,

$$\boldsymbol{\zeta}_{jn} := n^{-1/2}\sum_{t=1}^{n}\psi_\alpha(U_{jt})\mathbf{x}_{jt}, \quad U_{jt} := Y_t - \mathbf{x}_{jt}^T\boldsymbol{\beta}_j = \varepsilon_t - w_{jt}.$$

Therefore, $\sqrt{n}\,\mathrm{vec}[\hat{\boldsymbol{\beta}}_{jn} - \boldsymbol{\beta}_j] = \hat{\boldsymbol{\delta}}_n$ has the same asymptotic distribution as $\tilde{\boldsymbol{\delta}}_n$. Observe that the $\boldsymbol{\zeta}_{jn}$ are asymptotically jointly normal with $E(\boldsymbol{\zeta}_{jn}) = \mathbf{h}_{jn}$ and $\mathrm{Cov}(\boldsymbol{\zeta}_{jn}, \boldsymbol{\zeta}_{kn}) = \mathbf{C}_{jkn}$. Therefore, $\tilde{\boldsymbol{\delta}}_n \overset{A}{\sim} N(\boldsymbol{\mu}_n, \boldsymbol{\Sigma}_n)$, which proves the first assertion. As in the case of $q = 1$, the second assertion follows from the fact that $Z_{jn}(\hat{\boldsymbol{\delta}}_{jn}) = \tilde{Z}_{jn}(\tilde{\boldsymbol{\delta}}_{jn}) + o_P(1)$ and $\tilde{Z}_{jn}(\tilde{\boldsymbol{\delta}}_{jn}) = -(1/2)\boldsymbol{\zeta}_{jn}^T \boldsymbol{\Lambda}_{jn}^{-1} \boldsymbol{\zeta}_{jn}$.

Remark 1. One can relax the assumption (A5) by directly assuming that (a) $\sum_{t=1}^n \psi_\alpha(U_{jt})\mathbf{x}_{jt}$ has a central limit theorem and (b) $n^{-1}\sum_{t=1}^n \sum_{s=1}^n |\mathrm{Cov}\{\phi(U_{jt}, x), \phi(U_{js}, y)\}| = o(1)$ as $n \to \infty$, where $U_{jt} := Y_t - \mathbf{x}_{jt}^T \boldsymbol{\beta}_j$ and $\phi(u, x) := I(u \le x) - I(u < 0)$. Other relaxations of (A5) can be found in He and Shao (1996), Oberhofer and Haupt (2005), and Koenker (2005), for example.

Remark 2. The results can also be extended to the situation where the $\mathbf{x}_{jt}$ depend on n.

2. Proof of Theorem 1

First, consider the case where $\hat{\boldsymbol{\beta}}_n(\omega)$ is defined by (3). It suffices to apply the Quantile Regression Lemma to $Y_t - \lambda$ with $\mathbf{x}_{jt} := \mathbf{x}_t(\omega_j)$, $\boldsymbol{\beta}_j := 0$, and $c_t := 0$ so that $\hat{\boldsymbol{\beta}}_{jn} = \hat{\boldsymbol{\beta}}_n(\omega_j)$, $\varepsilon_t = Y_t - \lambda$, and $w_{jt} = 0$. Observe that $G_t(u) = F_t(\lambda + u)$ and $G_{ts}(u, v) = F_{ts}(\lambda + u, \lambda + v)$. This implies that $g_t(w_{jt}) = f_t(\lambda) = \kappa$ by (C2), so (A1) is satisfied. Similarly, (A2) is satisfied because by (C1),

$$G_t(u + w_{jt}) - G_t(w_{jt}) = F_t(\lambda + u) - F_t(\lambda) = f_t(\lambda)u + O(u^{d+1}) = g_t(w_{jt})u + O(u^{d+1}).$$

Moreover, let $\{\delta_j\}$ denote the Kronecker delta sequence. Because

$$n^{-1}\sum_{t=1}^n \mathbf{x}_t(\omega_j)\mathbf{x}_t^T(\omega_k) = \frac{1}{2}\delta_{j-k}\mathbf{I} + o(1), \tag{19}$$

it follows from (C2) that

$$\boldsymbol{\Lambda}_{jn} = n^{-1}\sum_{t=1}^n f_t(\lambda)\mathbf{x}_t(\omega_j)\mathbf{x}_t^T(\omega_j) = \frac{1}{2}\kappa\mathbf{I} + o(1),$$

so (A3) is satisfied. Furthermore, by (19), we can write

$$n^{-1}\sum_{t=\max(1,1+\tau)}^{\min(n,n+\tau)} \mathbf{x}_t(\omega_j)\mathbf{x}_{t-\tau}^T(\omega_k) = \frac{1}{2}\begin{bmatrix} \cos(\omega_j\tau) & -\sin(\omega_j\tau) \\ \sin(\omega_j\tau) & \cos(\omega_j\tau) \end{bmatrix}\delta_{j-k} + o(1).$$

In addition, by (C3), we have

$$r_{ts}(w_{jt}, w_{ks}) = F_{ts}(\lambda,\lambda) - F_t(\lambda)F_s(\lambda) = F_{ts}(\lambda,\lambda) - \alpha^2 = \alpha(1-\alpha) - (1/2)\gamma_{t-s}.$$

Combining these results leads to

$$\begin{aligned}\mathbf{C}_{jkn} &= n^{-1}\sum_{|\tau|<n}\{\alpha(1-\alpha)-(1/2)\gamma_\tau\}\sum_{t=\max(1,1+\tau)}^{\min(n,n+\tau)}\mathbf{x}_t(\omega_j)\mathbf{x}_{t-\tau}^T(\omega_k)\\ &= \frac{1}{2}\alpha(1-\alpha)S(\omega_j)\delta_{j-k}\mathbf{I}+o(1).\end{aligned}$$

Hence (A4) is also satisfied. Finally, under (C2), we obtain

$$\mathbf{h}_{jn} = n^{-1/2}\sum_{t=1}^{n}\{\alpha - F_t(\lambda)\}\mathbf{x}_t(\omega_j) = \mathbf{0}.$$

Therefore, an application of the Quantile Regression Lemma yields

$$\sqrt{n}\,\mathrm{vec}[\hat{\boldsymbol{\beta}}_n(\omega_j)]_{j=1}^q \overset{A}{\sim} N(\mathbf{0}, (2/\kappa^2)\alpha(1-\alpha)\mathbf{S}), \tag{20}$$

where $\mathbf{S} := \mathrm{diag}\{S(\omega_1), S(\omega_1), \ldots, S(\omega_q), S(\omega_q)\}$. This implies that the $Q_{n,\mathrm{I}}(\omega_j)$ are asymptotically independent and $Q_{n,\mathrm{I}}(\omega_j) \overset{A}{\sim} (1/2)\eta_{\mathrm{I}}^2 S(\omega_j)\chi_2^2$ for each j with $\eta_{\mathrm{I}}^2 := \alpha(1-\alpha)/\kappa^2$. Also by the Quantile Regression Lemma, we obtain

$$\sum_{t=1}^{n}\rho_\alpha(Y_t - \lambda - \mathbf{x}_t^T(\omega_j)\hat{\boldsymbol{\beta}}_n(\omega_j)) = \sum_{t=1}^{n}\rho_\alpha(Y_t-\lambda) - \frac{1}{2}\boldsymbol{\zeta}_{jn}^T\boldsymbol{\Lambda}_{jn}^{-1}\boldsymbol{\zeta}_{jn} + o_P(1),$$

where $\mathrm{vec}[\boldsymbol{\zeta}_{jn}]_{j=1}^q \overset{A}{\sim} N(\mathbf{0}, [\mathbf{C}_{jkn}])$. Therefore,

$$Q_{n,\mathrm{II}}(\omega_j) = \kappa^{-1}\|\boldsymbol{\zeta}_{jn}\|_2^2 + o_P(1), \quad \mathrm{vec}[\boldsymbol{\zeta}_{jn}]_{j=1}^q \overset{A}{\sim} N(\mathbf{0}, (1/2)\alpha(1-\alpha)\mathbf{S}).$$

This implies that the $Q_{n,\mathrm{II}}(\omega_j)$ are asymptotically independent and $Q_{n,\mathrm{II}}(\omega_j) \overset{A}{\sim} (1/2)\eta_{\mathrm{II}}^2 S(\omega_j)\chi_2^2$ for each j, where $\eta_{\mathrm{II}}^2 := \alpha(1-\alpha)/\kappa$.

Now consider the case where $\hat{\boldsymbol{\beta}}_n(\omega)$ is given by (6). In this case, we apply the Quantile Regression Lemma to Y_t with $\mathbf{x}_{jt} := [1, \mathbf{x}_t^T(\omega_j)]^T$, $\boldsymbol{\beta}_j := [\lambda, 0, 0,]^T$, and $c_t := \lambda$ so that $\hat{\boldsymbol{\beta}}_{jn} = [\hat{\lambda}_n(\omega_j), \hat{\boldsymbol{\beta}}_n^T(\omega_j)]^T$, $\varepsilon_t =$

$Y_t - \lambda$, and $w_{jt} = 0$. Similarly to the previous case, we have $G_t(w_{jt}) = F_t(\lambda) = \alpha$, $g_t(w_{jt}) = f_t(\lambda) = \kappa$, and $r_{ts}(w_{jt}, w_{ks}) = \alpha(1-\alpha) - (1/2)\gamma_{t-s}$. Moreover, combining (19) with $n^{-1}\sum_{t=1}^{n} \exp(it\omega_j) = o(1)$ yields

$$\mathbf{C}_{jkn} = \alpha(1-\alpha)\,\mathrm{diag}\{S(0), (1/2)S(\omega_j)\delta_{j-k}\mathbf{I}\} + o(1).$$

Similarly, we obtain $\mathbf{h}_{jn} = \mathbf{0}$ and

$$\mathbf{\Lambda}_{jn} = \kappa\,\mathrm{diag}\{1, (1/2)\mathbf{I}\} + o(1).$$

Therefore, by the Quantile Regression Lemma, the assertion (20) remains valid. Hence the resulting $Q_{n,\mathrm{I}}(\omega_j)$ have the same asymptotic distribution as in the previous case.

Moreover, the Quantile Regression Lemma also gives

$$\sum_{t=1}^{n} \rho_\alpha(Y_t - \hat{\lambda}_n(\omega_j) - \mathbf{x}_t^T(\omega_j)\hat{\boldsymbol{\beta}}_n(\omega_j) = \sum_{t=1}^{n} \rho_\alpha(Y_t - \lambda) - \frac{1}{2}\boldsymbol{\zeta}_{jn}^T \mathbf{\Lambda}_{jn}^{-1}\boldsymbol{\zeta}_{jn} + o_P(1),$$

where the $\boldsymbol{\zeta}_{jn}$ are asymptotically independent with

$$\boldsymbol{\zeta}_{jn} := n^{-1/2}\sum_{t=1}^{n} \psi_\alpha(Y_t - \lambda)\mathbf{x}_{jt} \overset{A}{\sim} N(\mathbf{0}, (1/2)\alpha(1-\alpha)\mathrm{diag}\{2S(0), S(\omega_j), S(\omega_j)\}).$$

Similarly, by applying the Quantile Regression Lemma to Y_t with $q := 1$, $\mathbf{x}_{1t} := 1$, $\boldsymbol{\beta}_1 := \lambda$, and $c_t := \lambda$, we obtain $\hat{\boldsymbol{\beta}}_{1n} = \hat{\lambda}_n$ and

$$\sum_{t=1}^{n} \rho_\alpha(Y_t - \hat{\lambda}_n) = \sum_{t=1}^{n} \rho_\alpha(Y_t - \lambda) - \frac{1}{2}\kappa^{-1}\zeta_n^2 + o_P(1),$$

where

$$\zeta_n := n^{-1/2}\sum_{t=1}^{n} \psi_\alpha(Y_t - \lambda) \overset{A}{\sim} N(0, \alpha(1-\alpha)S(0)).$$

Combining these results with (7) leads to

$$Q_{n,\mathrm{II}}(\omega_j) = \frac{1}{2}(\boldsymbol{\zeta}_{jn}^T \mathbf{\Lambda}_{jn}^{-1}\boldsymbol{\zeta}_{jn} - \kappa^{-1}\zeta_n^2) + o_P(1) = \kappa^{-1}\|\tilde{\boldsymbol{\zeta}}_{jn}\|_2^2 + o_P(1),$$

where $\tilde{\boldsymbol{\zeta}}_{jn} := n^{-1/2}\sum_{t=1}^{n} \psi_\alpha(Y_t - \lambda)\mathbf{x}_t(\omega_j) \overset{A}{\sim} N(\mathbf{0}, (1/2)\alpha(1-\alpha)S(\omega_j)\mathbf{I})$. Therefore, the $Q_{n,\mathrm{II}}(\omega_j)$ defined by (7) have the same asymptotic distribution as those defined by (5) in the previous case.

Remark 3. In light of Remark 2, the results can be generalized to the situation where the ω_j depend on n such that $n^{-1}\sum_{t=1}^{n}\mathbf{x}_t(\omega_j)\mathbf{x}_t^T(\omega_k) = (1/2)\delta_{j-k}\mathbf{I} + o(1)$.

3. Proof of Theorem 2

In the first case where $\hat{\boldsymbol{\beta}}_n(\omega_0)$ is given by (3), apply the Quantile Regression Lemma to $Y_t - \lambda$ with $q := 1$, $\mathbf{x}_{1t} := \mathbf{x}_t(\omega_0)$, $\boldsymbol{\beta}_1 := \boldsymbol{\beta}_0$, and $c_t := \lambda_t - \lambda$, so that $\hat{\boldsymbol{\beta}}_{1n} = \hat{\boldsymbol{\beta}}_n(\omega_0)$, $\varepsilon_t = Y_t - \lambda - c_t = Y_t - \lambda_t$, and $w_{1t} = 0$. Observe that $G_t(u) = F_t(\lambda_t + u)$ and $G_{ts}(u,v) = F_{ts}(\lambda_t + u, \lambda_s + v)$. Therefore, $G_t(w_{1t}) = F_t(\lambda_t) = \alpha$, $g_t(w_{1t}) = f_t(\lambda_t) = \kappa$, and $r_{ts}(w_{1t}, w_{1s}) = F_{ts}(\lambda_t, \lambda_s) - F_t(\lambda_t)F_s(\lambda_s) = \alpha(1-\alpha) - (1/2)\gamma_{t-s}$. This implies that

$$\mathbf{C}_{11n} = \frac{1}{2}\alpha(1-\alpha)S(\omega_0)\mathbf{I} + o(1), \quad \boldsymbol{\Lambda}_{1n} = \frac{1}{2}\kappa\mathbf{I} + o(1), \quad \mathbf{h}_{1n} = \mathbf{0}.$$

An application of the Quantile Regression Lemma gives

$$\sqrt{n}(\hat{\boldsymbol{\beta}}_n(\omega_0) - \boldsymbol{\beta}_0) \overset{A}{\sim} N(\mathbf{0}, (2/\kappa^2)\alpha(1-\alpha)S(\omega_0)\mathbf{I}).$$

Therefore, $Q_{n,\mathrm{I}}(\omega_0) \overset{A}{\sim} (1/2)\eta_{\mathrm{I}}^2 S(\omega_0)\chi_2^2(\theta_n)$, where $\theta_n := (1/2)n\|\boldsymbol{\beta}_0\|_2^2/(\eta_{\mathrm{I}}^2 S(\omega_0))$ is the noncentrality parameter of the chi-square distribution. Moreover, the Quantile Regression Lemma also gives

$$\sum_{t=1}^{n}\rho_\alpha(Y_t - \lambda - \mathbf{x}_t^T(\omega_0)\hat{\boldsymbol{\beta}}_n(\omega_0)) = \sum_{t=1}^{n}\rho_\alpha(Y_t - \lambda - \mathbf{x}_t^T(\omega_0)\boldsymbol{\beta}_0) - \kappa^{-1}\|\boldsymbol{\zeta}_n\|_2^2 + o_P(1),$$

where $\boldsymbol{\zeta}_n := n^{-1/2}\sum_{t=1}^{n}\psi_\alpha(Y_t - \lambda_t)\mathbf{x}_t(\omega_0) \overset{A}{\sim} N(\mathbf{0}, (1/2)\alpha(1-\alpha)S(\omega_0)\mathbf{I})$. Combining this result with (5) leads to

$$Q_{n,\mathrm{II}}(\omega_0) = \kappa^{-1}\|\boldsymbol{\zeta}_n\|_2^2 + \Delta_{n1} + o_P(1) \overset{A}{\sim} \frac{1}{2}\eta_{\mathrm{II}}^2 S(\omega_0)\chi_2^2 + \Delta_{n1},$$

where

$$\Delta_{n1} := \sum_{t=1}^{n}\{\rho_\alpha(Y_t - \lambda) - \rho_\alpha(Y_t - \lambda - \mathbf{x}_t^T(\omega_0)\boldsymbol{\beta}_0)\}.$$

Hence the assertion.

In the second case where $\hat{\boldsymbol{\beta}}_n(\omega_0)$ is given by (6), we apply the Quantile Regression Lemma to Y_t with $q := 1$, $\mathbf{x}_{1t} := [1, \mathbf{x}_t^T(\omega_0)]^T$, $\boldsymbol{\beta}_1 := [\lambda, \boldsymbol{\beta}_0^T]^T$, and $c_t := \lambda_t$, so that $\hat{\boldsymbol{\beta}}_{1n} = [\hat{\lambda}_n(\omega_0), \hat{\boldsymbol{\beta}}_n^T(\omega_0)]^T$, $\varepsilon_t = Y_t - \lambda_t$, and

$w_{1t} = 0$. It is easy to show that the resulting $Q_{n,\mathrm{I}}(\omega_0)$ has the same asymptotic distribution as in the first case. Moreover, the Quantile Regression Lemma also yields

$$\sum_{t=1}^{n} \rho_\alpha(Y_t - \hat{\lambda}_n(\omega_0) - \mathbf{x}_t^T(\omega_0)\hat{\boldsymbol{\beta}}_n(\omega_0)) = \sum_{t=1}^{n} \rho_\alpha(Y_t - \lambda - \mathbf{x}_t^T(\omega_0)\boldsymbol{\beta}_0) - \frac{1}{2}\boldsymbol{\zeta}_n^T \boldsymbol{\Lambda}_n^{-1} \boldsymbol{\zeta}_n + o_P(1),$$

where $\boldsymbol{\Lambda}_n = \kappa \,\mathrm{diag}\{1, (1/2)\mathbf{I}\} + o(1)$ and

$$\boldsymbol{\zeta}_n := n^{-1/2} \sum_{t=1}^{n} \psi_\alpha(Y_t - \lambda_t)\mathbf{x}_{1t} \overset{A}{\sim} N(\mathbf{0}, (1/2)\alpha(1-\alpha)\,\mathrm{diag}\{2S(0), S(\omega_0), S(\omega_0)\}).$$

Similarly, an application of the Quantile Regression Lemma to $Y_t - \mathbf{x}_t^T(\omega_0)\boldsymbol{\beta}_0$ with $q := 1$, $\mathbf{x}_{1t} := 1$, $\boldsymbol{\beta}_1 := \lambda$, and $c_t := \lambda$ leads to $\varepsilon_t = Y_t - \lambda_t$, $w_{1t} = 0$, and

$$\sum_{t=1}^{n} \rho_\alpha(Y_t - \tilde{\lambda}_n - \mathbf{x}_t^T(\omega_0)\boldsymbol{\beta}_0) = \sum_{t=1}^{n} \rho_\alpha(Y_t - \lambda - \mathbf{x}_t^T(\omega_0)\boldsymbol{\beta}_0) - \frac{1}{2}\kappa^{-1}\zeta_n^2 + o_P(1),$$

where $\zeta_n := n^{-1/2}\sum_{t=1}^{n} \psi_\alpha(Y_t - \lambda_t) \overset{A}{\sim} N(0, \alpha(1-\alpha)S(0))$ and

$$\tilde{\lambda}_n := \arg\min_{\lambda \in \mathbb{R}} \sum_{t=1}^{n} \rho_\alpha(Y_t - \lambda - \mathbf{x}_t^T(\omega_0)\boldsymbol{\beta}_0).$$

Combining these results with (7) yields

$$Q_{n,\mathrm{II}}(\omega_0) = \frac{1}{2}\kappa^{-1}\|\tilde{\boldsymbol{\zeta}}_n\|_2^2 + \Delta_{n2} + o_P(1) \overset{A}{\sim} \frac{1}{2}\eta_{\mathrm{II}}^2 S(\omega_0)\chi_2^2 + \Delta_{n2},$$

where $\tilde{\boldsymbol{\zeta}}_n := n^{-1/2}\sum_{t=1}^{n} \psi_\alpha(Y_t - \lambda_t)\mathbf{x}_t(\omega_0) \overset{A}{\sim} N(\mathbf{0}, (1/2)\alpha(1-\alpha)S(\omega_0)\mathbf{I})$ and

$$\Delta_{n2} := \sum_{t=1}^{n} \{\rho_\alpha(Y_t - \hat{\lambda}_n) - \rho_\alpha(Y_t - \tilde{\lambda}_n - \mathbf{x}_t^T(\omega_0)\boldsymbol{\beta}_0)\}.$$

Hence the assertion.

4. Proof of Equation (15)

Let W_1 and W_2 be jointly normal with mean 0 and variance 1. Let $r := E(W_1 W_2)$ be the autocorrelation coefficient. It is easy to verify that X_1 and X_2 given by the linear system of equations $X_1 = W_1$ and $rX_1 +$

$\sqrt{1-r^2}X_2 = W_2$ are distributed as i.i.d. $N(0,1)$ (Miwa, Hayter, and Kuriki 2003). Therefore,

$$\begin{aligned} P(W_1 \le c_1, W_2 \le c_2) &= P\Big\{X_1 \le c_1, rX_1 + \sqrt{1-r^2}X_2 \le c_2\Big\} \\ &= E\Big\{I(X_1 \le c_1)E\Big[rX_1 + \sqrt{1-r^2}X_2 \le c_2\Big|X_1\Big]\Big\} \\ &= E\Big\{I(X_1 \le c_1)\Phi\Big((c_2 - rX_1)/\sqrt{1-r^2}\Big)\Big\} \\ &= \int_{-\infty}^{c_1} \Phi\Big((c_2 - rx)/\sqrt{1-r^2}\Big)\phi(x)\,dx. \end{aligned}$$

Taking $W_1 := Y_{t+\tau}/\sigma$, $W_2 := Y_t/\sigma$, and $c_1 := c_2 := \lambda/\sigma$ yields (15) with $r = r_\tau$.

REFERENCES

Bloomfield, P. (2000), *Fourier Analysis of Time Series*, 2nd Edition, New York, Wiley.

Brockwell, P. J., and Davis, R. A. (1991), *Time Series: Theory and Methods*, 2nd Edition, New York: Springer.

Chung, K. L. (2001), *A Course in Probability Theory*, 3rd Edition, New York: Academic Press.

He, X. and Shao, Q. M., (1996), "A General Bahadur Representation of *M*-Estimators and Its Application to Linear Regression with Nonstochastic Designs," *Annals of Statistics*, 24, 2608–2630.

Knight, K. (1998), "Limiting Distributions for L_1 Regression Estimators Under General conditions," *Annals of Statistics*, 26, 755–770.

Koenker, R. (2005), *Quantile Regression*, Cambridge, UK: Cambridge University Press.

Li, T. H. (2008), "Laplace Periodogram for Time Series Analysis", *Journal of the American Statistical Association*, 103, 757–768. A complete version is available as IBM Research Report RC24473 at domino.research.ibm.com/library/cyberdig.nsf.

Li, T. H. (2010), "Robust Coherence Analysis in the Frequency Domain," *Proceedings of the European Signal Processing Conference (EURIPCO)*, 836–871.

Li, T. H. (2012), "On Robust Spectral Analysis by Least Absolute Deviations," *Journal of Time Series Analysis*, 33, 298–303.

Miwa, T., Hayter, A. J., and Kuriki, S. (2003), "The Evaluation of General Noncentred Orthant Probabilities," *Journal of the Royal Statistical Society*, Series B, 65, 223–234.

Oberhofer, W. and Haupt, H., (2005), "The Asymptotic Distribution of the Unconditional Quantile Estimator Under Dependence," *Statistics & Probability Letters*, 74, 243–250.

Pollard, D. (1991), "Asymptotics for Least Absolute Deviation Regression Estimators," *Econometric Theory*, 7, 186–199.

Portnoy, S. and Koenker, R. (1997), "The Gaussian Hare and the Laplacian Tortoise: Computability of Squared-Error Versus Absolute Error Estimators," *Statistical Science*, 12, 279–300.

Wise, G., Traganitis, A., and Thomas, J. (1977), "The Effect of a Memoryless Nonlinearity on the Spectrum of a Random Process," *IEEE Transactions on Information Theory*, 23, 84–89.